Evolution of Packets of Surface Gravity Waves over Strong Smooth Topography

By E. S. Benilov and C. P. Howlin

Wave packets in a smoothly inhomogeneous medium are governed by a nonlinear Schrödinger (NLS) equation with variable coefficients. There are two spatial scales in the problem: the spatial scale of the inhomogeneities and the distance over which nonlinearity and dispersion affect the packet. Accordingly, there are two limits where the problem can be approached asymptotically: when the former scale is much larger than the latter, and vice versa. In this paper, we examine the limit where the spatial scale of (periodic or random) inhomogeneities is much smaller than that of nonlinearity/dispersion (i.e., the latter effects are much weaker than the former). In this case, the packet undergoes rapid oscillations of the geometric-optical type, and also evolves slowly due to nonlinearity and dispersion. We demonstrate that the latter evolution is governed by an NLS equation with constant (averaged) coefficients. The general theory is illustrated by the example of surface gravity waves in a channel of variable depth. In particular, it is shown that topography increases the critical frequency, for which the nonlinearity coefficient of the NLS equation changes sign (in such cases, no steady solutions exist, i.e., waves with frequencies lower than the critical one disperse and cannot form packets).

1. Introduction

Problems involving solitary waves in media with smoothly varying properties arise in many areas of continuum mechanics. In physical oceanography, for

Address for correspondence: E. S. Benilov, Department of Mathematics, University of Limerick, Ireland; e-mail: Eugene.Benilov@ul.ie

STUDIES IN APPLIED MATHEMATICS 116:289–301

Published by Blackwell Publishing, 350 Main Street, Malden, MA 02148, USA, and 9600 Garsington Road, Oxford, OX4 2DQ, UK.

Table 1
Main Results on the Evolution of Solitary Waves Over Topography

	Limit (1)	Limit (2)
Shallow-water solitons	[2, 3]	[4]
Wave packets	[5]	Present paper

example, internal, surface, inertial, or Rossby waves are often affected by topography and/or varying currents. Similar problems are of interest for atmospheric sciences, seismology, etc.

Dynamics of a solitary wave in an inhomogeneous medium is associated with several spatial scales, such as the distance L_{nd}, which the wave needs to travel before nonlinearity or dispersion affects it, and the spatial scale L_t of the medium's inhomogeneity (we are particularly interested in water waves over an uneven bottom, so $_t$ stands for topography). In the general case, where $L_t \sim L_{nd}$, only numerical approach is possible (e.g., [1]), but for

$$L_t \gg L_{nd} \tag{1}$$

or

$$L_t \ll L_{nd}, \tag{2}$$

the problem can be approached asymptotically. In what follows, we shall also assume that the characteristic wavelength is much smaller than L_t, i.e., the medium is *smoothly* inhomogeneous.

Limit (1) has been first studied for surface gravity waves in a shallow channel of variable depth in [2, 3], see Table 1. It has been shown that, to leading order, the wave field can be represented by a KdV soliton, with its amplitude depending on the *current* value of the channel's depth. A similar problem for topography (2) has been considered in [4], where it was shown that the wave undergoes rapid oscillations of the geometric-optical type and also evolves slowly due to nonlinearity and dispersion. Assuming the topography to be periodic or random, [4] derived an asymptotic equation describing the slow evolution.

The above results have been partly extended in [5] from shallow-water solitons to wave packets, for surface gravity waves over topography (1). Topography (2) has yet to be examined in application to packets.[1]

[1] In addition to the papers cited above, [6] studied wave packets propagating over step-like topography of type (2). In this case, the wave passes over the bottom irregularity too quickly for nonlinearity and dispersion to interact with topography, which makes this case simpler than the periodic/random one. A similar setting [step-like topography of type (2)] has been examined by [7] for KdV solitons.

The present paper examines propagation of a wave packet over topography (2). In Sections 2–4, we formulate the problem, present an asymptotic analysis for periodic topography, and consider an example of such. In Section 5, we discuss random topography.

2. Formulation

Consider surface gravity waves in a plane channel of variable depth $H(x)$, where x is the horizontal coordinate (see Figure 1). Introducing the elevation $\eta\ (x,\ t)$ of the free surface (t is the time), we assume that all parameters and variables are nondimensionalized using by mean depth of the channel and acceleration due to gravity.

If the bottom is flat, the frequency ω and wavenumber k of a monochromatic wave are related by the dispersion relation,

$$\omega^2 = k \tanh kH. \tag{3}$$

This paper is concerned with *smooth* topography, such that the horizontal scale of $H(x)$ is much larger than the characteristic wavelength,

$$L_t \gg \langle k \rangle^{-1}, \tag{4}$$

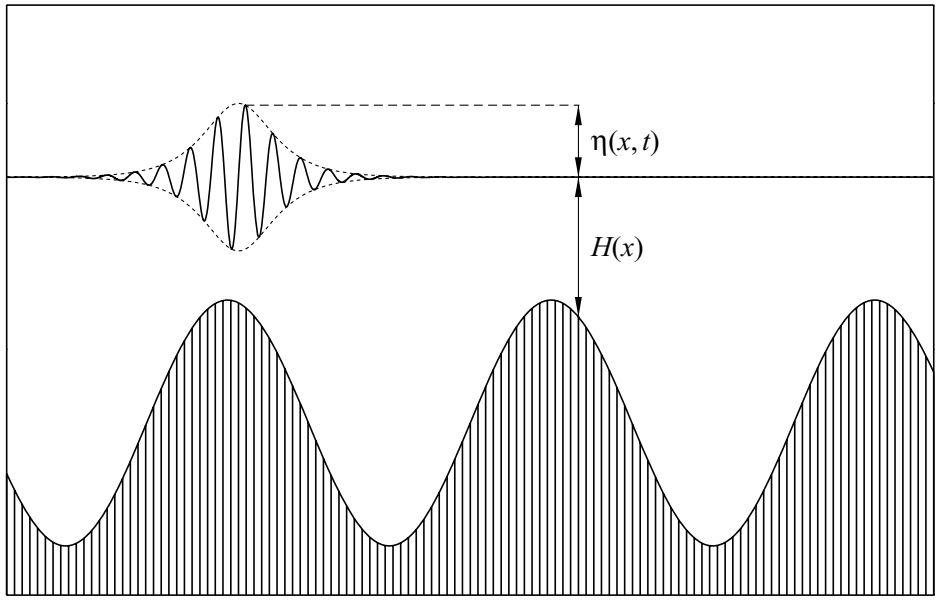

Figure 1. Formulation of the problem: a packet of surface gravity waves in a channel with topography.

where $\langle k \rangle$ is the characteristic wavenumber. In this case, we can introduce *quasimonochromatic* waves, i.e., such that

$$\eta(x,t) = \mathrm{Re}\left\{ A(x,t) \exp\left[\mathrm{i} \int k(x)\,\mathrm{d}x - \mathrm{i}\omega t \right] \right\}, \tag{5}$$

where A is a slowly changing function (its spatial/time scales exceed k^{-1} and ω^{-1}, respectively). Observe that the frequency ω in expression (5) is independent of x (which is always the case for linear or weakly nonlinear waves in media with stationary inhomogeneities, e.g., [8]), whereas the wavenumber varies in accordance with the dispersion relation (3).

The amplitude of the packet is governed by the nonlinear Schrödinger (NLS) equation derived in [6],

$$\mathrm{i}\left[\frac{\partial A}{\partial x} + \frac{1}{c_g(x)} \frac{\partial A}{\partial t} + \mu(x) A \right] + \alpha(x) \frac{\partial^2 A}{\partial t^2} + \beta(x) A |A|^2 = 0, \tag{6}$$

where

$$c_g = \frac{1}{2\omega} (\tanh kH + kH \,\mathrm{sech}^2 kH), \tag{7}$$

is the group velocity and

$$\mu = \frac{1}{2c_g} \frac{\mathrm{d}c_g}{\mathrm{d}x}, \tag{8}$$

$$\alpha = \frac{1}{2\omega c_g} \left(1 + \frac{2\omega H \tanh kH}{c_g} - \frac{H}{c_g^2} \right), \tag{9}$$

$$\beta = \frac{1}{2\omega^3 c_g} \left[3k^4 + 2\omega^4 k^2 - \omega^8 - \frac{\left(2k\omega + k^2 c_g \mathrm{sech}^2 kH \right)^2}{H - c_g^2} \right]. \tag{10}$$

Observe that relationship (8) guarantees that

$$\frac{\mathrm{d}}{\mathrm{d}x} \int_{-\infty}^{\infty} c_g |A|^2 \,\mathrm{d}t = 0,$$

which reflects conservation of the net energy flux.

Note also that Equation (6) is based on the assumption that the temporal spectrum of the solution is narrow-band (see [6]), whereas derivations of the standard NLS equation for *homogeneous* media are usually based on a similar assumption for the *spatial* spectrum. Accordingly, the role of the evolutionary variable in (6) is played by x, not t.

3. Wave packets over topography

It is convenient to change to a co-moving reference frame, i.e., replace t with

$$\tau = t - \int \frac{\mathrm{d}x}{c_g(x)}.$$

Then, in terms of (x, τ), the NSE equation (6) becomes

$$\mathrm{i}\frac{\partial}{\partial x}\left(c_g^{1/2}A\right) + c_g^{1/2}\left(\alpha\frac{\partial^2 A}{\partial\tau^2} + \beta A\,|A|^2\right) = 0. \tag{11}$$

In what follows, this equation will be examined asymptotically.

3.1. Asymptotic analysis

The problem at hand involves four spatial scales. In addition to the characteristic wavelength $\langle k\rangle^{-1}$ and the topographic scale L_t, we shall introduce the scales of nonlinearity and dispersion, L_n and L_d, representing the distances which a solitary wave needs to travel before these effects influence it. In terms of Equation (11), L_n and L_d can be determined by comparing the x-derivative with the last two terms, which yields

$$L_d = \frac{T_p^2}{\langle\alpha\rangle}, \quad L_n = \frac{1}{2\langle\beta\rangle|A_p|^2}, \tag{12}$$

where T_p and A_p are the packet's timescale and amplitude, $\langle\alpha\rangle$ and $\langle\beta\rangle$ are the characteristic values of the corresponding coefficients, and the factor of 2 in L_n has been introduced to make the two scales equal for a soliton over flat bottom (see formulae (30) below). We shall assume that nonlinearity and dispersion are of the same order, and are both weaker than topography, i.e.,

$$L_n, L_d \gg L_t. \tag{13}$$

Ordering (13) corresponds to the following change of variables:

$$\tilde{\tau} = \varepsilon^{1/2}t, \quad \tilde{A} = \varepsilon^{-1/2}A, \tag{14}$$

where

$$\varepsilon = \frac{L_t^2}{L_n^2} = \frac{L_t^2}{L_d^2}$$

is a small parameter. Substituting (14) into (11), we obtain (tildes omitted)

$$\mathrm{i}\frac{\partial}{\partial x}\left(c_g^{1/2}A\right) + \varepsilon c_g^{1/2}\left(\alpha\frac{\partial^2 A}{\partial\tau^2} + \beta A\,|A|^2\right) = 0. \tag{15}$$

To simplify this equation, we shall use the method of multiple scales, that is, in addition to x, introduce a slow spatial variable,

$$X = \varepsilon x,$$

and let

$$A(x, \tau) = A^{(0)}(x, X, \tau) + \varepsilon A^{(1)}(x, X, \tau) + \cdots.$$

To leading order, Equation (15) yields

$$\mathrm{i}\frac{\partial}{\partial x}\left(c_g^{1/2} A^{(0)}\right) = 0,$$

that is,

$$A^{(0)}(x, X, \tau) = c_g^{-1/2}(x)\, B(X, \tau), \tag{16}$$

where $B(X, \tau)$ is an undetermined function. Expression (16) is a typical geometric-optical result, reflecting conservation of the energy flux, $c_g |A^{(0)}|^2$, along a ray.

In the next order, we have

$$\mathrm{i}\frac{\partial}{\partial x}\left(c_g^{1/2} A^{(1)}\right) + \mathrm{i}\frac{\partial}{\partial X}\left(c_g^{1/2} A^{(0)}\right) + c_g^{1/2}\left(\alpha\frac{\partial^2 A^{(0)}}{\partial \tau^2} + \beta A^{(0)}\,|A^{(0)}|^2\right) = 0.$$

Assuming that $[A^{(1)}\ (x, X, \tau)]_{x=0} = 0$, we obtain

$$A^{(1)}(x, X, \tau) = \mathrm{i}c_g^{-1/2}(x)\int_0^x F(x', X, \tau)\,\mathrm{d}x', \tag{17}$$

where

$$F(x, X, \tau) = \mathrm{i}\frac{\partial}{\partial X}\left(c_g^{1/2} A^{(0)}\right) + c_g^{1/2}\left(\alpha\frac{\partial^2 A^{(0)}}{\partial \tau^2} + \beta A^{(0)}\,|A^{(0)}|^2\right). \tag{18}$$

Now, assume that $H(x)$ is periodic, and so is the function $F(x, X, \tau)$ with respect to the variable x. Then, to prevent $A^{(1)}$ from secular growth as $x \to \infty$, one has to require

$$\langle F \rangle = 0, \tag{19}$$

where $\langle \cdots \rangle$ denotes averaging with respect to x over one period of topography. Substituting (16) and (18) into (19), we obtain

$$\mathrm{i}\frac{\partial B}{\partial X} + \langle\alpha\rangle\frac{\partial^2 B}{\partial \tau^2} + \left\langle c_g^{-1}\beta\right\rangle B\,|B|^2 = 0. \tag{20}$$

This is an NLS equation with *constant* coefficients, which makes it much simpler than the original equation (11).

4. Examples

The asymptotic equation (20) has a two-parameter family of soliton solutions,

$$B(X,\tau) = \sqrt{\frac{2\langle\alpha\rangle}{\langle c_g^{-1}\beta\rangle}}\lambda \operatorname{sech}\left[\lambda(\tau - vX)\right] \times \exp\left\{\mathrm{i}\left[\frac{v\tau}{2\langle\alpha\rangle} + \left(\frac{v^2}{4\langle\alpha\rangle} - \langle\alpha\rangle^2\lambda^2\right)X\right]\right\}, \tag{21}$$

where λ and v are arbitrary real constants (the former determines the packet's amplitude and timescale, and the latter determines its velocity). In terms of the exact Equation (11), solution (21) corresponds to

$$A(x,\tau) \approx c_g^{-1/2}(x)\sqrt{\frac{2\langle\alpha\rangle}{\langle c_g^{-1}\beta\rangle}}\lambda \operatorname{sech}[\lambda(\tau - vx)] \times \exp\left\{\mathrm{i}\left[\frac{v\tau}{2\langle\alpha\rangle} + \left(\frac{v^2}{4\langle\alpha\rangle} - \langle\alpha\rangle\lambda^2\right)x\right]\right\}. \tag{22}$$

In order to verify that (22) is indeed an (asymptotic) solution, Equation (11) was solved numerically with the initial condition

$$A(0,\tau) = c_g^{-1/2}(0)\sqrt{\frac{2\langle\alpha\rangle}{\langle c_g^{-1}\beta\rangle}}\lambda \operatorname{sech}(\lambda\tau)\exp\left(\frac{\mathrm{i}v\tau}{2\langle\alpha\rangle}\right). \tag{23}$$

The nondimensional depth of the channel was assumed sinusoidal,

$$H(x) = 1 + \Delta H \sin\left(\frac{x}{L_t}\right), \tag{24}$$

where ΔH and L_t are the amplitude and spatial scale of the depth variation. We shall present results for

$$\Delta H = 0.6, \tag{25}$$

$$L_t = 5, \tag{26}$$

and for the following value of the initial wavenumber:

$$k = 2 \quad \text{at} \quad x = 0. \tag{27}$$

Substituting (24)–(27) into (3), we can compute $k(x)$, and then the characteristic wavelength,

$$\langle k\rangle^{-1} = 0.475. \tag{28}$$

The simulations were carried out for the following parameters of the wave packet:

$$\lambda = 0.1, \quad v = 0. \tag{29}$$

Before describing the numerical results, we shall demonstrate that the above values satisfy the restrictions of our asymptotic approach. To do so, observe that, as follows from (22), λ determines both the timescale and amplitude of the packet, which we shall define as follows:

$$T_p = \lambda^{-1}, \quad A_p = \left\langle c_g^{-1/2} \right\rangle \sqrt{\frac{2\langle\alpha\rangle}{\langle c_g^{-1}\beta\rangle}}\lambda.$$

Then, (12) yields the following expressions for the dispersion and nonlinearity scales:

$$L_d = \frac{1}{\langle\alpha\rangle\lambda^2}, \quad L_n = \frac{1}{\langle\alpha\rangle\lambda^2} \frac{\left\langle c_g^{-1}\beta \right\rangle}{\left\langle c_g^{-1/2} \right\rangle^2 \langle\beta\rangle}. \tag{30}$$

Observe that, for a soliton over flat bottom, the topographic factor in L_n cancels, resulting in $L_d = L_n$, i.e., dispersion and nonlinearity are in perfect balance.

Upon substitution of expressions (7), (9), and (10) for c_g, α, and β into (30), followed by a straightforward computation using the previously computed $k(x)$, we obtained

$$L_d = 92.0, \quad L_n = 114.1. \tag{31}$$

Equations (26), (28), and (31) show that assumptions (4) and (13) hold well.

The solution of the initial value problem (11), (23) was assumed periodic in τ, with a period that was sufficiently large to eliminate interaction of two successive solitary waves. The condition of periodicity allowed us to use the pseudo-spectral method for approximation of the τ-derivatives in Equation (11), and the Runge–Kutta scheme was used for the x-derivative. The results of simulations are presented in Figures 2 and 3.

Figure 2(a) shows the short-term evolution of the

$$\text{Relative amplitude of the packet} = \frac{\max\limits_{-\infty<\tau<\infty}\{|A(x,\tau)|\}}{\max\limits_{-\infty<\tau<\infty}\{A(0,\tau)\}}, \tag{32}$$

for parameters (27), (29), over the sinusoidal topography (24)–(26). One can see that the topography-induced oscillations are described by the asymptotic solution (22) well.

Compare also Figures 2(a) and (b) (the latter shows the topography profile), where two characteristic features are worth noting. Firstly, the packet's amplitude does *two* oscillations per *one* oscillation of topography; secondly, packet generally decays with decreasing depth and vice versa (which comes as

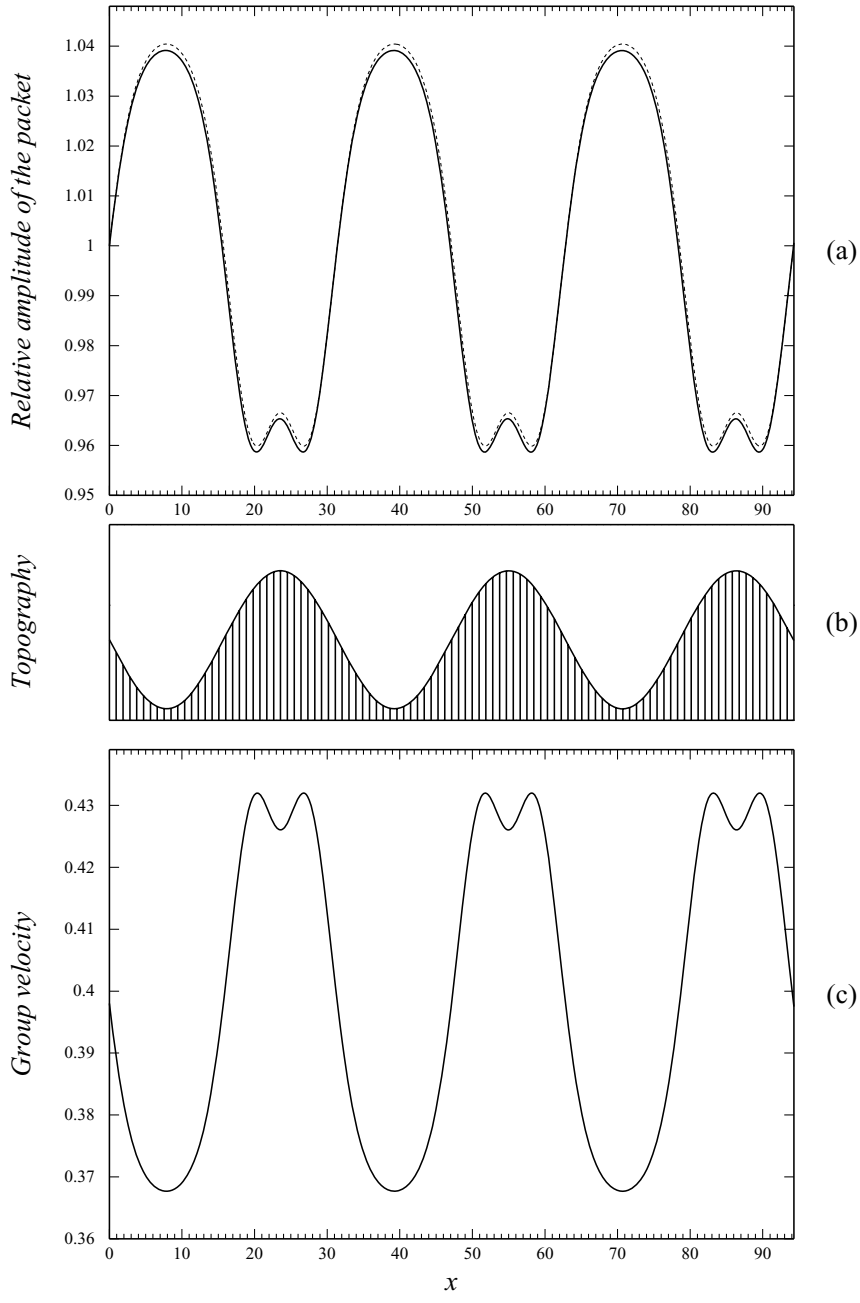

Figure 2. Short-term evolution of a wave packet (27), (29) over topography (24)–(26). (a) The relative amplitude of the wave packet [defined by (32)] vs. x. Solid line shows the numerical solution of the exact initial value problem (11), (23); dotted line shows the asymptotic solution (22). (b) The depth of the channel vs. x (the horizontal dashed line corresponds to $H = \omega^{-2}$). (c) The group velocity of the carrier wave vs. x.

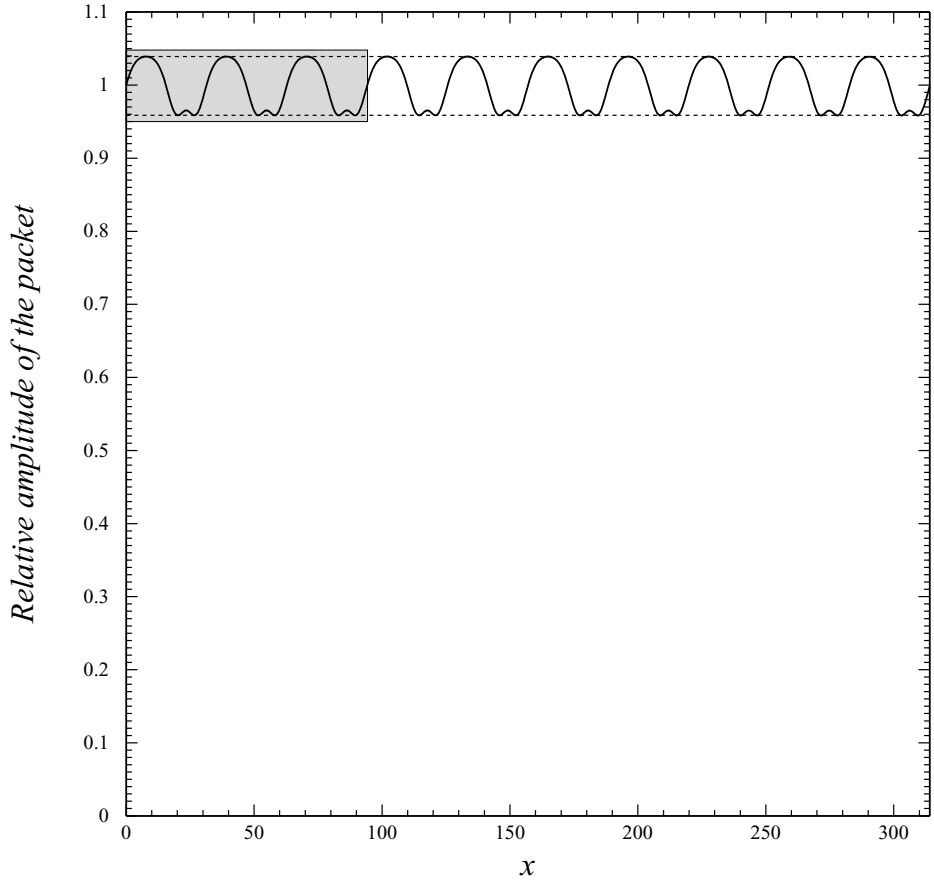

Figure 3. Long-term evolution of a wave packet (27), (29) over topography (24)–(26): the numerical solution of the exact initial value problem (11), (23). The shaded area corresponds to Figure 2(a), the dotted lines show the maximum and minimum values of the packet's amplitude and emphasize that these do not change from period to period.

a surprise, as one would expect a shoaling wave to amplify). Both features follow from the nonmonotonic dependence of the group velocity (and, hence, the wave's amplitude) on the channel's depth (it was first observed in [9]). Indeed, formulae (22) and (32) yield

$$\text{Relative amplitude of the packet} \approx \left[\frac{c_g(0)}{c_g(x)}\right]^{-1/2},$$

that is, the packet's amplitude has maxima at those points where $c_g(x)$ has minima and vice versa (compare Figures 2(a) and (c)). It is still unclear, however, why $c_g(x)$ has more than one minima per topography period, which can be clarified by differentiating expression (7) with respect to x,

$$\frac{\mathrm{d}c_g}{\mathrm{d}x} = \frac{\omega^2 \mathrm{sech}^2 kH}{(\omega^2 + H\mathrm{sech}^2 kH)^2}(1 - H\omega^2)\frac{\mathrm{d}H}{\mathrm{d}x}.$$

Now, one can see that $c_g(x)$ has extrema, where

$$H = \omega^{-2} \quad \text{or} \quad \frac{\mathrm{d}H}{\mathrm{d}x} = 0,$$

with the former points being maxima and the latter, minima (compare Figures 2(b) and (c)). This property of c_g explains the first feature of the evolution observed.

To explain the second feature, differentiate expression (7) with respect to H and use (3) to substitute for $\mathrm{d}k/\mathrm{d}H$, which yields

$$\frac{\mathrm{d}c_g}{\mathrm{d}H} = \frac{\mathrm{sech}^2(kH)(1 - H\omega^2)}{2c_g}.$$

Thus, if ω is sufficiently large, then $\mathrm{d}c_g/\mathrm{d}H < 0$, which corresponds to the packet's amplitude increasing with growing H, with the opposite behavior, the amplitude *decreasing* with H, occurring for *small* ω. Given that our intuition for water waves is mainly developed at beaches (where H, and hence ω, are small), the former case is the one we are less accustomed to, but is still quite possible.

The long-term evolution of the packet is illustrated in Figure 3, one can see that, apart from the topography-induced oscillations, the packet is steady. This agrees with the fact that the packet's *averaged* profile is a steady solution of the asymptotic equation (20) and confirms our asymptotic results.

An important property of equation (20) is associated with the dependence of its nonlinearity coefficient, $\langle c_g^{-1}\beta\rangle$, on the parameters of the carrier wave. For topography (24)–(26), for example, we have

$$\begin{aligned} k(0) = 2.0, \quad \omega = 1.389 \qquad & \langle c_g^{-1}\beta\rangle \approx 11.627, \\ k(0) = 1.9, \quad \omega = 1.348 \qquad & \langle c_g^{-1}\beta\rangle \approx 3.720, \\ k(0) = 1.8, \quad \omega = 1.305 \qquad & \langle c_g^{-1}\beta\rangle \approx -2.906. \end{aligned}$$

The change of the sign of the nonlinearity coefficient has important implications, because, in this case, Equation (20) has no soliton solutions. We emphasize that the case of flat bottom exhibits a similar property, but the *critical* parameter values, for which this occurs, are different. Indeed, assuming that $H = 1$ for all x, one can show that the nonlinearity coefficient, β, changes sign at

$$k \approx 1.363, \quad \omega \approx 1.093,$$

see [10].

5. Random topography

It appears that the asymptotic approach used in subsection 3.1 for periodic topography is equally applicable to a random one. Indeed, if $H(x)$ is statistically homogeneous with respect to shifting x, we only need to replace averaging over a period with averaging over the whole space.

It turns out, however, that, for random topography, condition (19) does *not* prevent $A^{(1)}$ from growth as $x \to \infty$.

To observe this, use solution (17) to calculate

$$\overline{A^{(1)}(x, X, \tau) A^{(1)*}(x, X, \tau)\, c_g(x)} = \int_0^x \int_0^x \overline{F(x', X, \tau)\, F^*(x'', X, \tau)}\, \mathrm{d}x'\, \mathrm{d}x'', \tag{33}$$

where the overbar denotes averaging over ensemble of realizations. Because spatial homogeneity of H entails a similar property for F, the integrand in (33) depends on $x' - x''$, not on x' and x'' separately,

$$\overline{F(x', X, \tau)\, F^*(x'', X, \tau)} = W(x' - x'').$$

Then,

$$\int_0^x \int_0^x W(x' - x'')\, \mathrm{d}x'\, \mathrm{d}x'' \to x \int_{-\infty}^{\infty} W(x')\, \mathrm{d}x' \quad \text{as} \quad x \to \infty, \tag{34}$$

where it is implied that the correlation function $W(x)$ decays sufficiently fast as $x \to \infty$, so the integral on the right-hand side of (34) converges.

Equalities (33) and (34) demonstrate that, if $\int_{-\infty}^{\infty} W(x')\, \mathrm{d}x' \neq 0$ (which is the general case), then

$$A^{(1)} = O(x^{1/2}) \quad \text{as} \quad x \to \infty.$$

Finally, comparing $\varepsilon A^{(1)}$ with the leading-order solution $A^{(0)}$, we conclude that our asymptotic method is valid only for

$$x \ll \varepsilon^{-2}. \tag{35}$$

Restrictions of the allowable distance similar to (35) are typical for asymptotic theories for media with random inhomogeneities. In similar problems, they have been observed in [4, 11]. Another paper, [12], considered wave packets in a basin of mean depth $\bar{H}$ with small non-smooth depth variations, i.e.,

$$|H - \bar{H}| \ll \bar{H}, \quad L_t \sim \langle k \rangle^{-1}.$$

However, the first-order solution was not tested for growth in this case.

6. Summary and concluding remarks

In this paper, we have examined the evolution of packets of surface gravity waves in a channel with topography, in the limit where the topographic scale is much smaller than those of nonlinearity/dispersion. It was shown that the amplitude of the packet is proportional to $c_g^{-1/2}(x)$ [see formula (22)] and, thus, undergoes fast spatial oscillations on the scale of the depth variation. Apart from this, the packet slowly evolves due to nonlinearity and dispersion, and a nonlinear Schrödinger equation (20), with constant (averaged) coefficients has been derived for the slow evolution. It was also shown that, in case random topography, the applicability of this equation is restricted by condition (35).

Finally, note that the results obtained in this work could be extended in two ways. Firstly, it would be interesting to compare them with a numerical simulation of the free-surface problem. Secondly, the present results need to be extended to topography depending on *both* horizontal coordinates, $H(x, y)$, which would enable one to apply them to a number of important problems of physical oceanography.

References

1. Y. Agnon, E. Pelinovsky, and A. Sheremet, Disintegration of cnoidal waves over smooth topography, *Stud. Appl. Math.* 101:49–71 (1998).
2. R. Grimshaw, The solitary wave in water of variable depth, *J. Fluid Mech.* 42:639–656 (1970).
3. L. A. Ostrovsky and E. N. Pelinovsky, Wave transformation on the surface of fluid of variable depth, *Izvestia, Atmospheric and Oceanic Physics* 6:552–555 (1970).
4. E. S. Benilov, On the surface waves in a shallow channel with an uneven bottom, *Stud. Appl. Math.* 87:1–14 (1992).
5. E. S. Benilov, J. D. Flanafgan, and C. P. Howlin, Evolution of packets of surface gravity waves over smooth topography, *J. Fluid Mech.* (2005).
6. V. D. Djordjević and L. G. Redekopp, On the development of packets of surface gravity waves moving over an uneven bottom, *J. Appl. Math. Phys. (ZAMP)* 29:950–962 (1978).
7. R. S. Johnson, Solitary wave, soliton and shelf evolution over variable depth, *J. Fluid Mech.* 276:125–138 (1994).
8. C. C. Mei, *The Applied Dynamics of Ocean Surface Waves*, Wiley, 1983.
9. W. Burnside, On the modification of a train of waves as it advances into shallow water, *Proc. Lond. Math. Soc.* 15:131–133 (1914).
10. T. B. Benjamin and J. E. Feir, The disintegration of wave trains on deep water. Part 1, *J. Fluid Mech.* 27:417–430 (1967).
11. E. S. Benilov and E. N. Pelinovsky, To the theory of nonlinear wave propagation in non–dispersive media with fluctuating parameters, *JETP* 94:175–185 (1988).
12. J. H. Pihl, C. C. Mei, and M. J. Hancock, Surface gravity waves over a two-dimensional random seabed, *Phys. Rev. E* 66:016611 (2002).

University of Limerick, Ireland

(Received April 11, 2005)